

# Morton curve segments produce no more than two distinct face-connected subdomains

Carsten Burstedde\*, Tobin Isaac†

December 3, 2024

## Abstract

The Morton- or  $z$ -curve is one example for a space filling curve: Given a level of refinement  $L \in \mathbb{N}_0$ , it maps the interval  $[0, 2^{dL}) \cap \mathbb{Z}$  one-to-one to a set of  $d$ -dimensional cubes of edge length  $2^{-L}$  that form a subdivision of the unit cube. In contrast to the Hilbert curve that is continuous, the Morton curve produces jumps. We prove that any contiguous subinterval of the curve divides the unit cube into no more than two face-connected, star-shaped subdomains, for arbitrary dimensions  $d > 0$ . In other words, there can be at most one jump in the curve that creates a new subdomain. We provide an algorithm for enumerating how many segments of a given length are continuous and prove a lower bound on the fraction of segments of a given length that are continuous. This result should eliminate concerns that the Morton curve may lead to an uncontrolled fragmentation of the domain.

## 1 Introduction

The Peano curve [15] and the Hilbert curve [11] are continuous maps from the line onto the  $d$ -dimensional unit cube. A large number of such space filling curves has been described in the literature; see for example [3, 10, 16] and the references therein. They are usually defined in terms of a recursive prescription. For numerical applications, the curve is made discrete and finite by bounding the depth of the recursion. The smallest units of space that are traversed are called elements. The Morton- or  $z$ -curve, originally described by Lebesgue [12] and adapted to data storage by Morton [14], also creates such a map, but it is not continuous. In fact, it contains jumps throughout its length (see Figure 1). This raises the concern that a subsection of the curve may divide the space covered by its image into a large number of disconnected subdomains. Especially when the curve is used to divide a computational mesh between different processors for parallel computation, see e.g. [1, 2, 5, 9, 18], such a property would likely increase the communication volume since the surface-to-volume ratio of a fragmented

---

\*Institut für Numerische Simulation (INS) and Hausdorff Center for Mathematics (HCM), Universität Bonn, Germany, [burstedde@ins.uni-bonn.de](mailto:burstedde@ins.uni-bonn.de) (corresponding author)

†Computing Institute, The University of Chicago, USA, [tisaac@ices.utexas.edu](mailto:tisaac@ices.utexas.edu)

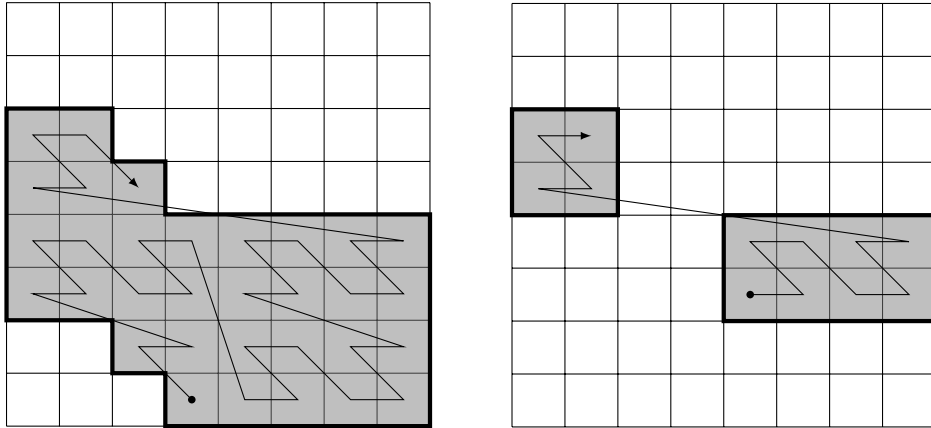


Figure 1: Contiguous subsections of the Morton curve at refinement level  $L = 3$ . Observe the jumps when the  $z$ -curve runs diagonally. In the right hand image, this produces two disconnected subdomains.

subdomain could grow without bounds. In this paper we eliminate this concern by proving that the Morton curve can lead to no more than two subdomains, where we define a set of elements to be of the same subdomain if they are connected by a finite number of element face connections.

We note that a proof has been given in [3, pages 175–177] that proceeds by illustrating and enumerating a finite number of cases in two dimensions. (In fact, we reiterate these ideas in dimensions two and three in Section 3, and also restate the extension to adaptive meshes in Section 5.) It is said in [3] that the construction extends to dimensions three and higher. This is entirely plausible, yet we see that the number of cases to discuss grows with the space dimension and would eventually require some kind of automation. Thus, in this work we develop formulas that are parametrized by an arbitrary dimension  $d$ . We complete our study with a statement on the lower bound on the fraction of continuous segments and provide an algorithm and numerical results to illustrate the distribution of continuous vs. discontinuous segments.

Last but not least, we provide alternative non-inductive proofs in the appendix by introducing certain formulas that operate on the Morton index. One byproduct is that we can prove that the connected segments are star-shaped.

## 2 Concepts and Notation

There is a natural identification between Morton-ordered elements on the one hand and uniform and adaptive quadtrees [8] and octrees [13] on the other. As outlined below, we often refer to the elements as (sub)quadrants irrespective of the space dimension  $d$ . Different ways exist to formalize the definition of a general space filling curve; one is to identify a finite set of types of transformations and rules to apply them recursively [10]. In this document we restrict the theory to the minimum required to treat the Morton curve.

The Morton subdivision of a  $d$ -dimensional hypercube [14] can be constructed

by recursion. When dividing a cube into  $2^d$  half-size subcubes, we enumerate these with the binary number

$$q = (q_d \dots q_1)_2 \in [0, 2^d) \cap \mathbb{Z} \quad (1)$$

comprised of  $d$  bits  $q_i \in \{0, 1\}$ . (We will drop  $\cap \mathbb{Z}$  in the following when it is clear that we are referring to integers.) Each of the bits  $i$  corresponds to the position of that subcube in the  $x_i$  coordinate direction, where 0 denotes the lower and 1 the higher half. In our convention the most significant bit corresponds to the last dimension ( $z$  in three dimensions) and the least significant bit to  $x \equiv x_1$ . When counting through the possible values of  $q$  we see that the  $x_1$  coordinate changes its value fastest and the  $x_d$  coordinate slowest. Before a bit at position  $i$  flips, all numbers in the lower  $i - 1$  bits have to be counted through first.

We can state one central and well known fact at this point: The flip of the  $i$ th bit amounts to a shift of the corresponding subcube parallel to the coordinate direction  $i$ . If we flip from zero to one, we move up, and else we move down the axis. It is easy to see that flipping one bit transforms the subcube into its neighbor across a face with normal direction  $\pm x_i$ .

We define a recursion by subdividing each subcube further using the same prescription. The root cube is associated with level  $\ell = 0$ , with levels increasing with each subdivision. Subcubes exist at any level  $\ell$  and are identified with the root of a corresponding subtree. Level- $L$  subtrees are also called subquadrants. We count the sequence of level  $L$  (sub)quadrants with the index

$$Q = (q^1 \dots q^L)_2 \in [0, 2^{dL}), \quad (2)$$

where the level-wise indices  $q^\ell$  are defined as in (1). Each of them designates a choice of subquadrant from the first subdivision  $\ell = 1$  to the last at level  $\ell = L$ . This sequence of choices can be understood as the path from the root to the leaf of a decision tree, where each decision is between  $2^d$  possibilities. The subset of  $\mathbb{R}^d$  occupied by the quadrant with index  $Q$  is

$$\begin{aligned} \Omega(Q) := & [2^{-L}(q_1^1 q_1^2 \dots q_1^L)_2, 2^{-L}((q_1^1 q_1^2 \dots q_1^L)_2 + 1)] \times \\ & [2^{-L}(q_2^1 q_2^2 \dots q_2^L)_2, 2^{-L}((q_2^1 q_2^2 \dots q_2^L)_2 + 1)] \times \\ & \vdots \\ & [2^{-L}(q_d^1 q_d^2 \dots q_d^L)_2, 2^{-L}((q_d^1 q_d^2 \dots q_d^L)_2 + 1)]. \end{aligned} \quad (3)$$

We define a full or complete subtree by the set of all its descendant quadrants. A subtree is incomplete if the quadrants form a subset of descendants that are contiguous with respect to the indexing (2). We call such a subset a segment of a Morton curve in the following (two examples are depicted in Figure 1).

We will make use of the following symmetry property of the Morton curve: It can be traversed forward or in reverse. The reversal amounts to go through the indexing (2) by counting backwards. A quadrant is transformed into the reverse ordering by taking the bitwise negation (the one-complement) of its index,

$$R(Q) = 2^{dL} - 1 - Q. \quad (4)$$

Geometrically, this operation mirrors the quadrant around the center point of the root cube.



Figure 2: We show two  $L = 2$  examples of Morton curve segments that begin with the first subquadrant of a tree (left) and end with its last subquadrant (right), respectively. In both cases the segment covers one face-connected subdomain.

### 3 Illustrated Proofs for $d \leq 3$

In this section we prove a set of statements for up to three dimensions by providing selected illustrations and covering all possible cases. A similar argument has been explored before in two dimensions [3], while an abstract proof for two dimensions can be found in [7]. We provide abstract proofs for arbitrary dimension  $d$  later in Section 4 that do not rely on the present section and are in fact more concise; the reader may jump forward if so inclined.

We begin with statements that assume a curve that either begins with the first subquadrant of the unit cube or ends with its last subquadrant. In a second step, we use these statements to prove the final result. All statements are stated for arbitrary levels of refinement  $L \geq 0$ . In fact, all statements are trivially true for one dimension  $d = 1$  (with no jumps at all); in this section we cover  $d = 2$  and  $d = 3$ .

**Proposition 1.** *In a quadtree (or octree)  $T$  that is uniformly refined to level  $L$ , a contiguous segment of a Morton curve that begins with the first subquadrant in  $T$  creates exactly one subdomain of face-connected quadrants, no matter where it ends.*

**Corollary 2.** *In the situation of Proposition 1, a contiguous segment that ends with the last subquadrant in  $T$  creates exactly one face-connected subdomain, no matter where it begins (see Figure 2 for an illustration).*

*Proof.* Assuming that Proposition 1 is true, we can use the symmetry of the  $z$ -curve with respect to reversal to transform the present problem into the setting covered in Proposition 1.  $\square$

*Proof of Proposition 1.* We proceed by induction over  $L$ . Starting with  $L = 0$ , we only have one element and the statement is true. Supposing  $L > 0$ , we can identify the number  $j \in [0, 2^d)$  that designates in which level 1 subquadrant of the tree the last level  $L$  subquadrant of the segment lies. If  $j = 0$  then the whole segment is contained in a level  $L - 1$  subtree and we can apply the induction assumption. Each of the remaining cases produces  $j$  full subtrees and one possibly incomplete one. That last subtree necessarily contains its first level  $L$  subquadrant  $q$ . Since this subtree produces one subdomain by induction, we

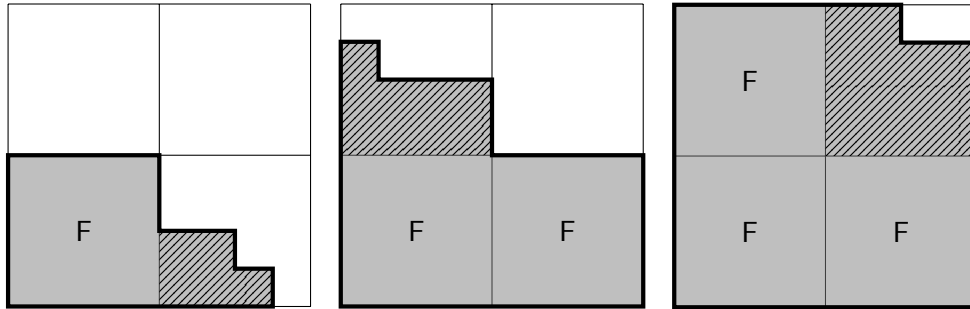


Figure 3: Proof of Proposition 1: The three non-trivial cases that occur in two dimensions (we choose  $L = 3$ ). The letter  $F$  designates a fully covered subtree of level  $L - 1$ . It is crucial that the lower left corner of the hatched area touches at least one of the full subtrees across a face.

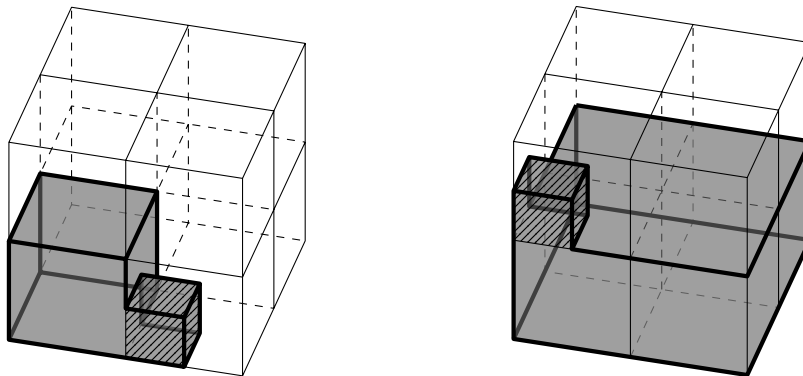


Figure 4: Proof of Proposition 1: Selected cases in three dimensions ( $j = 1, 4$  out of the seven non-trivial ones). The full subtrees are shaded lightly. Again we exploit the fact that the lower left front corner of the last non-empty subtree (hatched) connects to at least one full subtree with a lower subtree index across a face.

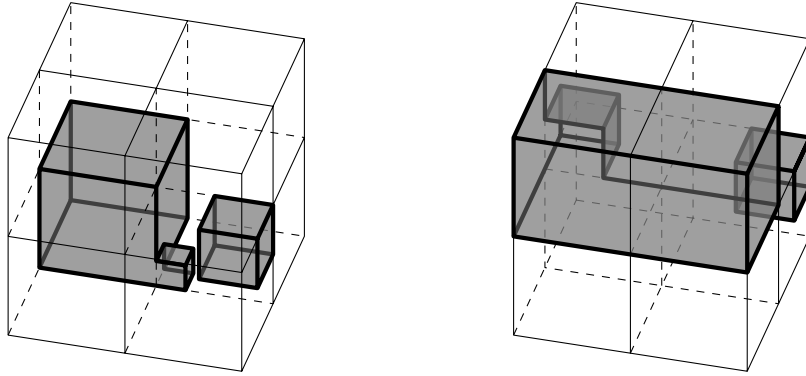


Figure 5: The cases 1–3 and 3–6 in the proof of Proposition 3 for  $d = 3$  dimensions. Each of these examples produces two distinct face-connected subdomains.

are done by arguing that the full subtrees are face-connected to each other and to  $q$ , directly or indirectly. For two dimensions we show the three possible cases in Figure 3, all of which satisfy the statement. For three dimensions we proceed by enumeration as well; we show selected situations in Figure 4 to conclude the proof.  $\square$

Now that we have identified situations that produce one subdomain only, we can prove the main statement for arbitrary segments by a divide-and-conquer approach.

**Proposition 3.** *In a quadtree or octree that is uniformly refined to level  $L$ , a contiguous segment of the Morton curve creates no more than two distinct face-connected subdomains.*

*Proof.* We proceed by induction over  $L$ . Again, the case  $L = 0$  leaves nothing to prove. If the segment of the curve is contained in one level  $L-1$  subtree, the proof is finished by induction. Else we have one subtree in which the segment begins, zero to  $2^d - 2$  fully covered subtrees, and one subtree in which the segment ends. To the first nonempty subtree we can apply Corollary 2, while Proposition 1 applies to the last one. Thus we know that the possibly incomplete subtrees lead to one connected piece each. The case of two nonempty subtrees is thus completed and it remains to consider three or more.

Now, whenever any two adjacent nonempty subtrees have even-odd numbers, they are face-connected since at least one of them must be full. This covers the remaining three- and four-subtree cases in two dimensions. In three dimensions, this clears all situations with three non-empty subtrees. Since we can further reduce the number of remaining cases by symmetry, it remains to examine the subtree ranges  $(i, \dots, i+3)$  through  $(i, \dots, 7)$  for  $i = 0, \dots, 3$ . All of these cases satisfy our claim; we illustrate a few in Figure 5.  $\square$

We have completed the necessary proofs for a uniform space division in  $d \leq 3$ . In the next section we provide a proof for arbitrary dimension  $d$ . The case of adaptive space divisions is considered in Section 5.

## 4 Proofs for Arbitrary Dimension

In this section we use induction over both the dimension and the level of subdivision to prove the main statement for all dimensions  $d > 0$  (non-recursive proofs are provided in Appendix A). These proofs imply the statements of the previous Section 3 as special cases. For convenience we denote any  $d$ -tant as a quadrant. We make use of the following definition of subtree ranges.

**Definition 4.** *Let the space dimension be  $d > 0$ . For any  $0 \leq d' \leq d$  and  $0 \leq k < 2^{d-d'}$ , we define the following interval containing  $2^{d'}$  integers,*

$$I_k^{d'} = 2^{d'}[k, k + 1). \quad (5)$$

*We use this interval to denote a specific contiguous range of subtree indices.*

We define the following auxiliary statements, first considering a one-sided segment and then a general two-sided one.

**Proposition 5.** *If a segment of a Morton curve is fully contained in the level 1 subtrees enumerated by a given  $I_k^{d'}$  and contains the first or last subquadrant in this range of subtrees, then it corresponds to one face-connected subvolume.*

*Proof.* By symmetry of the Morton curve, we can restrict the discussion to the case of the first subquadrant. Let us begin by proving the statement for subdivision level  $L = 1$ . By (5) the lowest subtree index in the segment is  $k2^{d'}$ . This number has  $d'$  zero bits from the right. All other indices in  $I_k^{d'}$  have one or more ones in the lower  $d'$  bits while being bitwise identical in the higher bits. For any of these indices we can flip the low bits to zero one by one, effectively transitioning through face neighbors and monotonously decreasing the index until we reach  $k2^{d'}$ . This whole sequence of face-connected subtrees is contained in  $I_k^{d'}$ . In conclusion, all trees in  $I_k^{d'}$  are face-connected to  $k2^{d'}$  and thus to each other.

Now let  $L > 1$  and assume the above statement for  $L - 1$ . To prove it for  $L$  we make an induction over  $d'$ . If  $d' = 0$  we have a single subtree and can readily invoke the induction assumption for  $L - 1$ . Else there are two possible cases: Either the segment is fully contained in one of  $I_{2k}^{d'-1}$  or  $I_{2k+1}^{d'-1}$  and we apply the induction over  $d'$ . Otherwise  $I_{2k}^{d'-1}$  contains full subtrees only and the segment reaches into  $I_{2k+1}^{d'-1}$ . Each nonempty subtree  $j$  in the latter interval must contain its first subquadrant, which has a face connection to the full tree  $j - 2^{d'-1} \in I_{2k}^{d'-1}$ . Since by the proof for  $L = 1$  all subtrees in  $I_{2k}^{d'-1}$  are face-connected, we are done.  $\square$

**Proposition 6.** *If a segment of a Morton curve is contained in the level 1 subtrees  $I_k^{d'}$ , it produces no more than two distinct face-connected subvolumes.*

*Proof.* Again let us prove the statement first for  $L = 1$ . If  $d' = 0$  we have just one level 1 subquadrant that clearly satisfies our claim. For positive  $d'$  we distinguish the following cases. If the segment is fully contained in either  $I_{2k}^{d'-1}$  or  $I_{2k+1}^{d'-1}$ , we apply the induction on  $d'$ . Else we know that the last subquadrant

of  $I_{2k}^{d'-1}$  and the first of  $I_{2k+1}^{d'-1}$  are in the segment. By Proposition 5 we have at most two disconnected pieces and the statement holds.

If  $L > 1$  the case  $d' = 0$  reduces to the same statement for  $L - 1$  and we are done by applying the induction over  $L$ . Else, the proof proceeds unchanged as above with the desired result.  $\square$

We have implicitly proved the main result for any uniform level  $L$  subdivision, since a level 0 subtree trivially satisfies our claim, and otherwise the root cube is the union of the level 1 subtrees  $I_0^d$ .

## 5 Main Statement

We have completed the necessary proofs for a uniform space division, for any number of space dimensions  $d$ . As we state in this section, an adaptive space division does not require any more effort (see also [3, page 176]).

**Theorem 7.** *A contiguous segment of a Morton curve through a uniform or adaptive tree of maximum refinement level  $L$  produces at most two distinct face-connected subdomains.*

*Proof.* Any adaptive tree of quadrants with level  $\leq L$  can be refined into level  $L$  quadrants exclusively. This operation does not change the connectivity between boundaries of the designated subdomain. In particular, the number of face-connected subdomains remains unchanged and the proof reduces to applying Propositions 3 (only  $d \leq 3$ ) or 6 (any  $d$ ) above.  $\square$

Finally, when we consider a forest of octrees as in [4, 6, 17], we must consider the case when a contiguous segment of the Morton curve traverses more than one tree. In this case, the segment necessarily contains the last subquadrant of any predecessor tree, as well as the first subquadrant of any successor tree in the segment. By Proposition 5 we know that no jumps can occur at all (when not counting the transition between two successive trees as a jump).

## 6 Enumeration of Face-Connected Segments

Having shown that a segment of a Morton curve is composed of one or two face-connected subdomains, a natural question to ask is how many each type there are. More formally, we ask: for a given dimension  $d$ , recursive level  $L$ , and segment length  $l$ , what fraction  $\phi_{d,L,l}$  of the  $2^{dL} - (l - 1)$  possible segments are in one face-connected piece?

This question can be answered recursively. Each segment of length  $l > 1$  on level  $L$  can refine to  $2^{2d}$  segments on level  $(L+1)$  with lengths between  $2^d(l-2)+2$  and  $2^{d+1}l$ , as illustrated in Figure 6. We divide connected segments into two categories: weakly connected, when the first and last quadrants in the segment are (face-)adjacent, and strongly connected, when they are not. Disconnected segments only refine to disconnected segments. Strongly connected segments only refine to strongly connected segments. Weakly connected segments refine

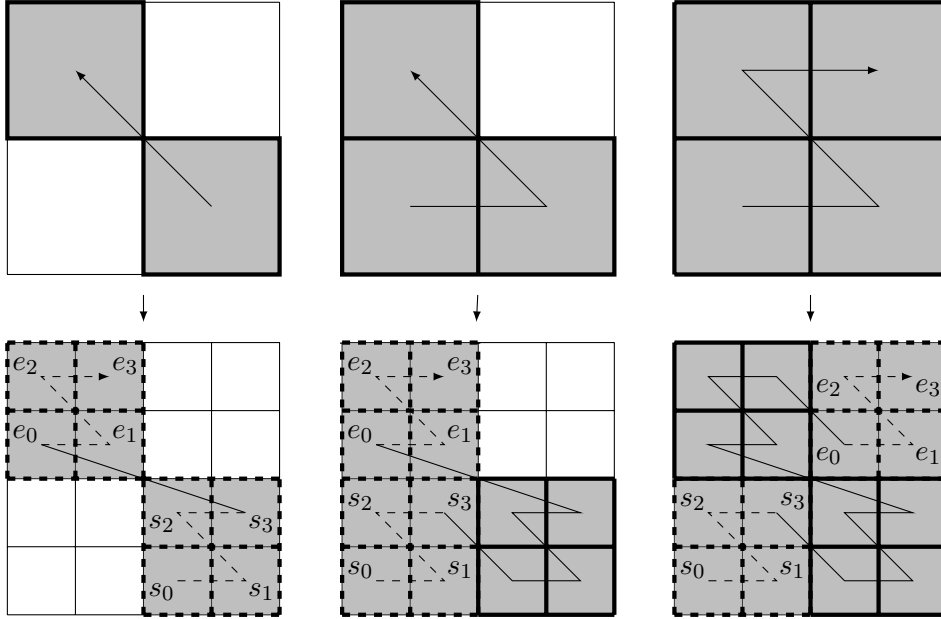


Figure 6: The refinement of disconnected (left), weakly connected (middle), and strongly connected segments (right). Each coarse segment (top) refines to one of  $2^{2d} = 16$  possible refined segments (bottom), each starting with  $s \in \{s_0, \dots, s_3\}$  and ending with  $e \in \{e_0, \dots, e_3\}$ . Disconnected segments refine to disconnected segments; strongly connected segments refine to strongly connected segments; weakly connected segments refine to disconnected (e.g.,  $\{s_3, \dots, e_0\}$ ), weakly connected (e.g.,  $\{s_2, \dots, e_0\}$ ), and strongly connected segments (e.g.,  $\{s_0, \dots, e_3\}$ ).

to all three types: how many of each depends on the direction in which the first and last quadrants are adjacent.

We give pseudocode for this recursive calculation in the function `Enumerate` (Algorithm 1). This algorithm is implemented in the Python script `morton.py`.<sup>1</sup>

`Enumerate` calls on some lookup tables: `RefineOne( $d, l$ )` (Figure 7) counts how many disconnected, strongly and weakly connected segments of length  $l$  are refined from one  $d$ -dimensional quadrant (the weakly connected segments are broken down by the direction in which the first and last quadrant are adjacent); `RefineWeak( $d, j, r$ )` (Figure 8) counts how many disconnected, strongly and weakly connected segments with  $r$  quadrants in the end-families are refined from one weakly connected segment in direction  $j$  (a weakly connected segment only produces weakly connected segments in the same direction).

In Figure 9, we use `Enumerate` to calculate the fraction of connected segments  $\phi_{d,L,l}$  for  $d = 2$  and  $d = 3$  for large values of  $L$ . We observe that  $\phi_{d,L,l}$  tends to vary between  $1/2$  and  $1/(2^d - 1)$ . In Appendix B, we prove that the latter is indeed a lower bound.

<sup>1</sup><https://github.com/cburststede/p4est/tree/develop/doc/morton/morton.py>

---

**Algorithm 1:** Enumerate ( $d, L, l$ )

---

**Data:** dimension  $d \geq 1$ , level  $L \geq 0$ , segment length  $1 \leq l \leq 2^{dL}$ .

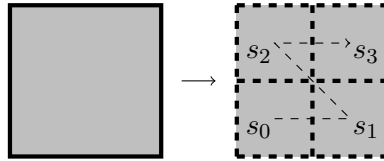
**Result:**  $(n_d, n_s, n_{w,1}, \dots, n_{w,d})$ , the number of segments of length  $l$  that are disconnected, strongly connected, and weakly connected in each direction.

```

1 if  $l = 1$  or  $L = 0$  then    [define segments of length 1 to be strongly connected]
2   | return  $(0, 2^{dL}, 0, \dots, 0)$     [one segment for each quadrant]
3 end
4  $(n_d, n_s, n_{w,1}, \dots, n_{w,d}) \leftarrow (0, \dots, 0)$ 
5  $c \leftarrow \lceil l/2^d \rceil$     [compute the shortest length that can refine to length  $l$ ]
6 if  $l \bmod 2^d < 2$  then  $C \leftarrow 1 + \lfloor l/2^d \rfloor$  else  $C \leftarrow 2 + \lfloor l/2^d \rfloor$     [... longest ...]
7 for  $k \in \{c, \dots, C\}$  do
8   | if  $k = 1$  then
9     |  $N \leftarrow 2^{d(L-1)}$     [# of coarse quadrants]
10    |  $(n_d, n_s, n_{w,1}, \dots, n_{w,d}) \leftarrow (n_d, n_s, n_{w,1}, \dots, n_{w,d}) + N * \text{RefineOne}(d, l)$ 
11   | else
12     |  $r \leftarrow l - (k - 2)2^d$     [# of children in two coarse end quadrants]
13     |  $m \leftarrow \min\{(r - 1), 2^{d+1} - (r - 1)\}$  [# of ways to split between two families]
14     |  $(N_d, N_s, N_{w,1}, \dots, N_{w,d}) \leftarrow \text{Enumerate}(d, L - 1, k)$ 
15     |  $n_d \leftarrow n_d + N_d * m$     [disconnected  $\rightarrow$  disconnected]
16     |  $n_s \leftarrow n_s + N_s * m$     [strongly connected  $\rightarrow$  strongly connected]
17     | for  $1 \leq j \leq d$  do
18     |   |  $(n_d, n_s, n_{w,j}) \leftarrow (n_d, n_s, n_{w,j}) + N_{w,j} * \text{RefineWeak}(d, j, r)$ 
19     |   | end
20   | end
21 end
22 return  $(n_d, n_s, n_{w,1}, \dots, n_{w,d})$ 

```

---



RefineOne(2,1)	$n_s = 4 (\{s_0\}, \{s_1\}, \{s_2\}, \{s_3\})$
RefineOne(2,2)	$n_d = 1 (\{s_1, s_2\}), n_{w,1} = 2 (\{s_0, s_1\}, \{s_2, s_3\})$
RefineOne(2,3)	$n_{w,2} = 2 (\{s_0, s_1, s_2\}, \{s_1, s_2, s_3\})$
RefineOne(2,4)	$n_s = 1 (\{s_0, s_1, s_2, s_3\})$

Figure 7: We list the RefineOne( $d, l$ ) tables used in Enumerate (Algorithm 1) for  $d = 2$  as an example. Unlisted values are zero.

RefineWeak(2,2,2)	$n_d = 1$ ( $\{s_3, \dots, e_0\}$ )
RefineWeak(2,2,3)	$n_{w,2} = 2$ ( $\{s_2, \dots, e_0\}, \{s_3, \dots, e_1\}$ )
RefineWeak(2,2,4)	$n_s = 3$ ( $\{s_1, \dots, e_0\}, \{s_2, \dots, e_1\}, \{s_3, \dots, e_2\}$ )
RefineWeak(2,2,5 $\leq r \leq 8$ )	$n_s = 9 - r$ ( $\{s_0, \dots, e_{r-5}\}, \dots, \{s_{8-r}, \dots, e_3\}$ )

Figure 8: We list the RefineWeak( $d, j, r$ ) tables used in Enumerate (Algorithm 1) for  $d = 2$  and  $j = 2$  as an example. The start points and end points refer to Figure 6 (middle). Unlisted values are zero.

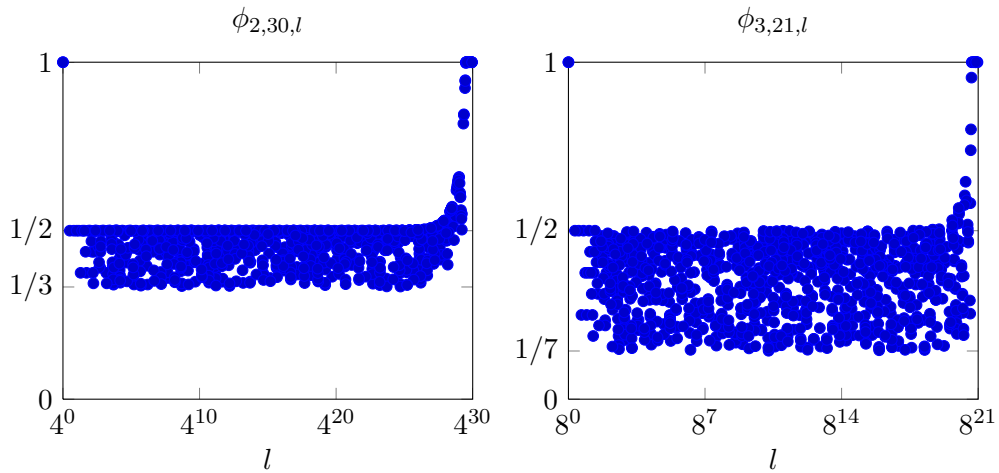


Figure 9: We plot the fraction of continuous segments of length  $l$ ,  $\varphi_{d,L,l}$ , for  $d = 2$  and  $L = 30$ , (left) and  $d = 3$  and  $L = 21$  (right), for one thousand log-uniformly randomly sampled lengths.

## 7 Conclusion

We prove in this document that the Morton curve does not lead to a fragmentation of the root cube into more than two disconnected subdomains. Its loss of continuity in comparison to the Hilbert curve is thus controlled. This is in line with experimental results, some of which we cite in Section 1, that establish the suitability of the Morton curve for numerical applications.

In conclusion, our result appears relevant to make informed choices about the type of space filling curve to use, for example in writing a new element-based parallel code for the numerical solution of partial differential equations, or any other code that benefits from a recursive subdivision of space.

## Acknowledgements

B. would like to thank Andreas Dedner for the invitation to the ICMS workshop on Galerkin methods with applications in weather and climate forecasting, which provided motivation to finally work on this conjecture. We would like to thank Michael Bader, Herman Haverkort, and Johannes Holke for suggesting additional relevant literature. B. gratefully acknowledges the support of the Hausdorff Center for Mathematics (HCM) at Bonn University and the collaborative research initiative Transregio 32, both supported by the German Research Foundation (DFG). I. gratefully acknowledges the support of the Intel Parallel Computing Center at the University of Chicago.

## References

- [1] A. AHIMIAN, I. LASHUK, S. VEERAPANENI, C. APARNA, D. MALHOTRA, I. MOON, R. SAMPATH, A. SHRINGARPURE, J. VETTER, R. VUDUC, D. ZORIN, AND G. BIROS, *Petascale direct numerical simulation of blood flow on 200k cores and heterogeneous architectures*, in SC10: Proceedings of the International Conference for High Performance Computing, Networking, Storage, and Analysis, ACM/IEEE, 2010. (Gordon Bell Prize).
- [2] V. AKÇELIK, J. BIELAK, G. BIROS, I. EPANOMERITAKIS, A. FERNANDEZ, O. GHATTAS, E. J. KIM, J. LOPEZ, D. R. O'HALLARON, T. TU, AND J. URBANIC, *High resolution forward and inverse earthquake modeling on terascale computers*, in SC03: Proceedings of the International Conference for High Performance Computing, Networking, Storage, and Analysis, ACM/IEEE, 2003. Gordon Bell Prize for Special Achievement.
- [3] M. BADER, *Space-Filling Curves: An Introduction with Applications in Scientific Computing*, Texts in Computational Science and Engineering, Springer, 2012.
- [4] W. BANGERTH, R. HARTMANN, AND G. KANSCHAT, *deal.II – a general-purpose object-oriented finite element library*, ACM Transactions on Mathematical Software, 33 (2007), p. 24.

- [5] C. BURSTEDDE, O. GHATTAS, M. GURNIS, T. ISAAC, G. STADLER, T. WARBURTON, AND L. C. WILCOX, *Extreme-scale AMR*, in SC10: Proceedings of the International Conference for High Performance Computing, Networking, Storage and Analysis, ACM/IEEE, 2010. Gordon Bell Prize finalist.
- [6] C. BURSTEDDE, L. C. WILCOX, AND O. GHATTAS, *p4est: Scalable algorithms for parallel adaptive mesh refinement on forests of octrees*, SIAM Journal on Scientific Computing, 33 (2011), pp. 1103–1133.
- [7] M. DE BERG, H. HAVERKORT, S. THITE, AND L. TOMA, *Star-quadtrees and guard-quadtrees: I/O-efficient indexes for fat triangulations and low-density planar subdivisions*, Computational Geometry, 43 (2010), pp. 493–513.
- [8] R. A. FINKEL AND J. L. BENTLEY, *Quad trees A data structure for retrieval on composite keys*, Acta Informatica, 4 (1974), pp. 1–9.
- [9] M. GRIEBEL AND G. W. ZUMBUSCH, *Parallel multigrid in an adaptive PDE solver based on hashing and space-filling curves*, Parallel Computing, 25 (1999), pp. 827–843.
- [10] H. HAVERKORT AND F. VAN WALDERVEEN, *Locality and bounding-box quality of two-dimensional space-filling curves*, Computational Geometry, 43 (2010), pp. 131–174.
- [11] D. HILBERT, *Über die stetige Abbildung einer Linie auf ein Flächenstück*, Mathematische Annalen, 38 (1891), pp. 459–460.
- [12] H. L. LEBESGUE, *Leçons sur l'intégration et la recherche des fonctions primitives*, Gauthier-Villars, 1904.
- [13] D. MEAGHER, *Geometric modeling using octree encoding*, Computer Graphics and Image Processing, 19 (1982), pp. 129–147.
- [14] G. M. MORTON, *A computer oriented geodetic data base; and a new technique in file sequencing*, tech. rep., IBM Ltd., 1966.
- [15] G. PEANO, *Sur une courbe, qui remplit toute une aire plane*, Math. Ann., 36 (1890), pp. 157–160.
- [16] H. SAGAN, *Space-Filling Curves*, Springer, 1994.
- [17] J. R. STEWART AND H. C. EDWARDS, *A framework approach for developing parallel adaptive multiphysics applications*, Finite Elements in Analysis and Design, 40 (2004), pp. 1599–1617.
- [18] T. WEINZIERL AND M. MEHL, *Peano—a traversal and storage scheme for octree-like adaptive Cartesian multiscale grids*, SIAM Journal on Scientific Computing, 33 (2011), pp. 2732–2760.

## A Alternative Proofs on Face Connectivity

These proofs do not rely on induction, but only on the map  $\Omega$  from index  $Q = (q^1 \dots q^L)_2$  to a subset of  $\mathbb{R}^d$  given in (3). For  $1 \leq r \leq d$ , we define the coordinate along axis  $r$ ,

$$Q_r = (q_r^1 \dots q_r^L)_2. \quad (6)$$

The map  $\Omega(Q)$  may be written as

$$\Omega(Q) = [2^{-L}Q_1, 2^{-L}(Q_1 + 1)] \times \dots \times [2^{-L}Q_d, 2^{-L}(Q_d + 1)]. \quad (7)$$

**Lemma 8.** *If  $Q$  and  $\tilde{Q}$  are such that  $\tilde{Q}_k \leq Q_k$  for all  $1 \leq k \leq d$ , then  $\tilde{Q} \leq Q$ .*

*Proof.* The order of the bits in  $Q_k$  ( $\tilde{Q}_k$ ) is the same as their order in  $Q$  ( $\tilde{Q}$ ).  $\square$

**Theorem 9.** *For any index  $Q^{\text{end}}$ , the interior of  $Y_0 = \cup_{Q=0}^{Q^{\text{end}}} \Omega(Q)$  is star-shaped (and thus  $Y_0$  is face-connected and contractible).*

*Proof.* If  $Q \in \{0, \dots, Q^{\text{end}}\}$ , then so are all  $\tilde{Q}$  such that  $\tilde{Q}_k \leq Q_k$  for all  $1 \leq k \leq d$ . The domains of these quadrants define a box between the origin and the corner of  $\Omega(Q)$  farthest from the origin,

$$B(Q) := [0, 2^{-L}(Q_1 + 1)] \times \dots \times [0, 2^{-L}(Q_d + 1)]. \quad (8)$$

Indeed,  $Y_0$  is the union of these boxes,  $Y_0 = \cup_{Q=0}^{Q^{\text{end}}} B(Q)$ , and the union of their interiors is the interior of  $Y_0$ . Each of these boxes contains the midpoint of  $\Omega(0)$  in its interior and is star-shaped with respect to it. Therefore the interior of  $Y_0$  is star-shaped with respect to that point as well.  $\square$

**Corollary 10.** *If  $Q|Q^{\text{start}} = Q$  ( $|$  means bitwise-or) for all  $Q \in \{Q^{\text{start}}, \dots, Q^{\text{end}}\}$ , then the interior of  $Y = \cup_{Q=Q^{\text{start}}}^{Q^{\text{end}}} \Omega(Q)$  is star-shaped.*

*Proof.* If  $Q|Q^{\text{start}} = Q$ , then the 1-bits of  $Q - Q^{\text{start}}$  are a subset of the 1-bits of  $Q$ . One can then verify that  $(Q - Q^{\text{start}})_k = Q_k - Q_k^{\text{start}}$  for all  $1 \leq k \leq d$ . Therefore  $\cup_{Q=Q^{\text{start}}}^{Q^{\text{end}}} \Omega(Q - Q^{\text{start}})$  is  $Y$  translated by the vector  $(-2^{-L}Q_1^{\text{start}}, \dots, -2^{-L}Q_d^{\text{start}})$ . This is the same as  $\cup_{Q=0}^{Q^{\text{end}} - Q^{\text{start}}} \Omega(Q)$ , which is star-shaped by Theorem 9.  $\square$

**Corollary 11.** *If  $Q \& Q^{\text{end}} = Q$  ( $\&$  means bitwise-and) for all  $Q \in \{Q^{\text{start}}, \dots, Q^{\text{end}}\}$ , then the interior of  $Y$  is star-shaped.*

*Proof.* Mirroring every quadrant about the midpoint of the unit cube does not change the shape of  $Y$ . The mirror of  $\Omega(Q)$  is  $\Omega(R(Q))$ , where  $R(Q)$  denotes the bitwise negation (4). Therefore  $R(Q)|R(Q^{\text{end}}) = R(Q \& Q^{\text{end}}) = R(Q)$  for all  $R(Q) \in \{R(Q^{\text{end}}), \dots, R(Q^{\text{start}})\}$ .  $\square$

**Theorem 12.** *The interior of  $Y$  is star-shaped, or  $Y$  is the union of two sets whose interiors are star-shaped.*

*Proof.* Let  $\tilde{q}$  be the most significant bits common to all of  $\{Q^{\text{start}}, \dots, Q^{\text{end}}\}$ . We can split the segment into  $\{Q^{\text{start}}, \dots, (\tilde{q}011 \dots 1)_2\}$  and  $\{(\tilde{q}100 \dots 0)_2, \dots, Q^{\text{end}}\}$ . The interior of the domain of the first segment is star-shaped by Corollary 11; the interior of the domain of the second segment is star-shaped by Corollary 10.  $\square$

## B Lower Bound on Fraction of Continuous Segments

**Theorem 13.** *The fraction of continuous segments of length  $l$  of the level- $L$   $d$ -dimensional Morton curve is*

$$\phi_{d,L,l} \geq \frac{1}{2^d - 1}. \quad (9)$$

*Proof.* Let  $s = \{Q^{\text{start}}, \dots, Q^{\text{end}} = Q^{\text{start}} + l - 1\}$  be the first discontinuous segment of length  $l$ . As in the proof of Theorem 12,  $s$  divides into two continuous segments,  $\{Q^{\text{start}}, \dots, (\tilde{q}011\dots 1)_2\}$  and  $\{(\tilde{q}100\dots 0)_2, \dots, Q^{\text{end}}\}$ , where  $\tilde{q}$  are significant bits that are common to all numbers in the segment. By the same reasoning as used in Corollary 10, the shapes of the two segments are not affected by  $\tilde{q}$ : changing  $\tilde{q}$  translates the whole domain. Therefore, as this is the first discontinuous segment,  $\tilde{q}$  must be  $(0\dots 0)$ , i.e., the two continuous pieces of the segment are  $s^- = \{Q^{\text{start}}, \dots, 2^k - 1\}$  and  $s^+ = \{2^k, \dots, Q^{\text{end}}\}$  for some  $k$ . Since  $Q^{\text{end}}$  cannot have a more significant 1-bit than  $2^k$ ,  $Q^{\text{end}} \leq 2^{k+1} - 1$ . We note that bitwise negation of the first  $k+1$  bits,  $\tilde{R}(Q) := 2^{k+1} - 1 - Q$ , induces a map  $\Omega(Q) \mapsto \Omega(\tilde{R}(Q))$  that is the reflection about the midpoint of the box formed by  $\cup_{Q=0}^{2^{k+1}-1} \Omega(Q)$ .

We first want to find a lower bound for  $Q^{\text{start}}$ . We note that  $2^k \in s^+$ , so if  $\Omega(Q^*)$  is a face neighbor of  $\Omega(2^k)$ , then  $Q^* \notin s^-$ , and if  $Q^* < 2^k$ , then because of the definition of  $s^-$ ,  $Q^*$  is less than every  $Q \in s^-$ , including  $Q^{\text{start}}$ . Let  $j = k \bmod d$  and let  $j' = d - j - 1$ . The  $Q^*$  that plays the crucial role is the neighboring quadrant that is closer to the origin in the  $(j+1)$ th direction. We have to subtract one from the  $(j+1)$ th coordinate of  $2^k$ : i.e.,  $(2^k)_{j+1} = 2^{\lfloor k/d \rfloor}$  in the notation of (6), so  $Q^*_{j+1} = 2^{\lfloor k/d \rfloor} - 1$ , while the other coordinates are the same, viz. zero. Therefore

$$\begin{aligned} Q^* &= (0\dots 0 \underbrace{0\dots 0}_{j'\text{-times}} \underbrace{10\dots 0}_{j\text{-times}})_2 &= \sum_{i=1}^{\lfloor k/d \rfloor} 2^{(i-1)d+j} \\ &= \sum_{i=1}^{\lfloor k/d \rfloor} 2^{(\lfloor k/d \rfloor - i)d+j} &= 2^k \sum_{i=1}^{\lfloor k/d \rfloor} 2^{-id} \\ &= 2^k \left( \sum_{i=1}^{\infty} 2^{-id} - \sum_{i=\lfloor k/d \rfloor + 1}^{\infty} 2^{-id} \right) &= 2^k \frac{1}{2^d - 1} - 2^k \sum_{i=\lfloor k/d \rfloor + 1}^{\infty} 2^{-id} \\ &= 2^k \frac{1}{2^d - 1} - 2^j \sum_{i=1}^{\infty} 2^{-id} &= \frac{2^k - 2^j}{2^d - 1}. \end{aligned} \quad (10)$$

By the definition of  $Q^{\text{start}}$ , there is a continuous segment of length  $l$  that starts at each  $Q \in \{0, \dots, Q^*\}$ . For each of these continuous segments, there is another continuous segment, obtained by the reflection map  $\tilde{R}$ , than ends with  $Q \in \{\tilde{R}(Q^*), \dots, 2^{k+1} - 1\}$ . We want to show that these two sets of continuous segments are distinct, i.e., that there is no segment of length  $l$  that starts with  $Q \leq Q^*$  and ends with  $Q + l - 1 \geq \tilde{R}(Q^*)$ . We thus have to show that the

shortest segment with endpoints in each set,  $\{Q^*, \dots, \tilde{R}(Q^*)\}$  is longer than  $l$ , i.e.,  $l < \tilde{R}(Q^*) - Q^* + 1 = 2^{k+1} - 2Q^*$ .

We will prove this bound by finding an upper bound for  $Q^{\text{end}}$ . We note that  $\tilde{R}(2^k) = 2^k - 1 \in s^-$ , so  $\Omega(\tilde{R}(Q^*))$  is a face neighbor of  $\Omega(2^k - 1)$ , so by the same reasoning as above,  $\tilde{R}(Q^*)$  must be greater than  $Q^{\text{end}}$ , and thus

$$l = Q^{\text{end}} - Q^{\text{start}} + 1 \leq (\tilde{R}(Q^*) - 1) - (Q^* + 1) + 1 = 2^{k+1} - 2Q^* - 2. \quad (11)$$

We have shown that there are at least  $2(Q^* + 1)$  continuous segments in the first  $2^{k+1}$  segments, each of which begins and ends in the range  $\{0, \dots, 2^{k+1} - 1\}$ . None of the numbers in these segments has more than  $k + 1$  significant bits, so by the same reasoning as in Corollary 10, adding a multiple of  $2^{k+1}$  to each number in one of these segments is a translation of its domain, and is thus continuous. Therefore there are at least  $2(Q^* + 1)$  continuous segments for *every*  $2^{k+1}$  segments, and thus

$$\begin{aligned} \phi_{d,L,l} &\geq \frac{2(Q^* + 1)}{2^{k+1}} = \frac{Q^* + 1}{2^k} \\ &= \frac{2^k - 2^j}{2^k(2^d - 1)} + \frac{1}{2^k} \\ &= \frac{2^k - 2^j + 2^d - 1}{2^k(2^d - 1)} \\ &\geq \frac{2^k}{2^k(2^d - 1)} \quad [j < d \text{ by definition}] \\ &= \frac{1}{2^d - 1}. \end{aligned} \quad (12)$$

□